Since January 2020 Elsevier has created a COVID-19 resource centre with free information in English and Mandarin on the novel coronavirus COVID-19. The COVID-19 resource centre is hosted on Elsevier Connect, the company's public news and information website.

Life Sciences 293 (2022) 120284

Contents lists available at ScienceDirect

Life Sciences

journal homepage: www.elsevier.com/locate/lifescie

ACE2 internalization induced by a SARS-CoV-2 recombinant protein is modulated by angiotensin II type 1 and bradykinin 2 receptors

Andrea Estefanía Portales [a], Emilio Román Mustafá [a], Clara Inés McCarthy [a], María Paula Cornejo [b], Paula Monserrat Couto [c], Mariela Mercedes Gironacci [d], Julio Javier Caramelo [c], Mario Perelló [b], Jesica Raingo [a,*]

[a] Laboratorio de Electrofisiología, Instituto Multidisciplinario de Biología Celular (IMBICE), Universidad Nacional de La Plata (UNLP), Consejo Nacional de Investigaciones Científicas y Técnicas (CONICET) and Comisión de Investigaciones Científicas de la Provincia de Buenos Aires (CIC), Calle 526 1499-1579, B1906APM Tolosa, Buenos Aires, Argentina.
[b] Laboratorio de Neurofisiología, Instituto Multidisciplinario de Biología Celular (IMBICE), Universidad Nacional de La Plata (UNLP), Consejo Nacional de Investigaciones Científicas y Técnicas (CONICET) and Comisión de Investigaciones Científicas de la Provincia de Buenos Aires (CIC), Calle 526 1499-1579, B1906APM Tolosa, Buenos Aires, Argentina.
[c] Fundación Instituto Leloir and Instituto de Investigaciones Bioquímicas de Buenos Aires, Consejo Nacional de Investigaciones Científicas y Técnicas (CONICET), Argentina.
[d] Universidad de Buenos Aires, Facultad de Farmacia y Bioquímica, Instituto de Química y Fisicoquímica Biológicas (IQUIFIB, UBA-CONICET), Argentina.

ARTICLE INFO

Keywords:
SARS-CoV-2
ACE2
AT1R
B2R
Telmisartan
Angiotensin II

ABSTRACT

Aims: Angiotensin-converting enzyme 2 (ACE2) is a key regulator of the renin-angiotensin system (RAS) recently identified as the membrane receptor for the severe acute respiratory syndrome coronavirus 2 (SARS-CoV-2). Here we aim to study whether two receptors from RAS, the angiotensin receptor type 1 (AT1R) and the bradykinin 2 receptor (B2R) modulate ACE2 internalization induced by a recombinant receptor binding domain (RBD) of SARS-CoV-2 spike protein. Also, we investigated the impact of ACE2 coexpression on AT1R and B2R functionality.

Materials and methods: To study ACE2 internalization, we assessed the distribution of green fluorescent protein (GFP) signal in HEK293T cells coexpressing GFP-tagged ACE2 and AT1R, or B2R, or AT1R plus B2R in presence of RBD alone or in combination with AT1R or B2R ligands. To estimate ACE2 internalization, we classified GFP signal distribution as plasma membrane uniform GFP (PMU-GFP), plasma membrane clustered GFP (PMC-GFP) or internalized GFP and calculated its relative frequency. Additionally, we investigated the effect of ACE2 coexpression on AT1R and B2R inhibitory action on voltage-gated calcium channels ($Ca_V2.2$) currents by patch-clamp technique.

Key findings: RBD induced ACE2-GFP internalization in a time-dependent manner. RBD-induced ACE2-GFP internalization was increased by angiotensin II and reduced by telmisartan in cells coexpressing AT1R. RBD-induced ACE2-GFP internalization was strongly inhibited by B2R co-expression. This effect was mildly modified by bradykinin and rescued by angiotensin II in presence of AT1R. ACE2 coexpression impacted on B2R- and AT1R-mediated inhibition of $Ca_V2.2$ currents.

Significance: Our work contributes to understand the role of RAS modulators in the susceptibility to SARS-CoV-2 infection and severity of COVID-19.

1. Introduction

Angiotensin-converting enzyme 2 (ACE2) is a key counterbalancing enzyme of the renin-angiotensin system (RAS) that catalyzes the conversion of the pressor hormone angiotensin II (Ang II) into the protective angiotensin 1–7 (Ang 1–7) [1]. Ang II acts through the angiotensin II type 1 receptor (AT1R) and causes vasoconstriction, apoptosis, inflammation and fibrosis. In contrast, Ang1–7 acts via the Mas receptor (MasR) and causes vasodilation as well as anti-inflammatory and anti-proliferative effects [2–4]. The interest on ACE2 research was renewed

* Corresponding author.
E-mail address: jraingo@imbice.gov.ar (J. Raingo).

https://doi.org/10.1016/j.lfs.2021.120284
Received 29 October 2021; Received in revised form 20 December 2021; Accepted 27 December 2021
Available online 14 January 2022

with the outbreak of the coronavirus infectious disease 2019 (COVID-19) since this cell surface enzyme was identified as the main receptor for the severe acute respiratory syndrome coronavirus 2 (SARS-CoV-2) entrance into host alveolar type II epithelial cells [5–7]. Similar to other viruses, SARS-CoV-2 takes advantage of the cellular endocytic machinery to initiate the infection [8]. The spike protein (S protein) anchored to the viral envelope binds to ACE2 through its receptor-binding domain (RBD) [9], and the SARS-CoV-2/ACE2 complex is then internalized mostly by a clathrin-dependent pathway [10,11]. Since each viral particle entering the cell is attached to an ACE2 molecule, it has been speculated that SARS-CoV-2 infection causes partial or total loss of ACE2 function on the cell surface with the consequent accumulation of Ang II and reduction in Ang 1–7 levels [12–16]. Such dysregulation of the RAS in lungs and at the systemic level has been proposed to favor a pro-inflammatory state that increases the severity of COVID-19 [17–20].

Some studies indicate that AT1R modulates ACE2 internalization [21,22]. AT1R activity is associated with the development of hypertension, among other medical conditions [23–27]. Interestingly, hypertension is a well-established risk factor for severe outcomes of COVID-19 [28–32], and Ang II is known to enhance ACE2 internalization through an AT1R dependent-mechanism [21,22]. Although such evidence suggests AT1R as an important player in the disease, its role in SARS-CoV-2 infection has been little explored [33]. G protein-coupled receptors (GPCRs), such as AT1R, interact with other receptors or proteins to form heteromers altering their functionality [34–37]. Since AT1R interacts with ACE2 [21,22], AT1R interactions with other GPCRs in the plasma membrane could influence ACE2 availability to mediate SARS-CoV-2 infection. The bradykinin B2 receptor (B2R) pathway promotes vasorelaxation, acting as a physiological antagonist of the Ang II-AT1R pathway [38,39]. Growing evidence shows that B2R can heteromerize with AT1R [40–43] and, thus, emerges as a candidate to modulate ACE2 surface density. The binding of ligands to GPCRs is another element that could modify GPCRs interactions with other proteins [44]. Endogenous and synthetic ligands are available for AT1R and B2R [23,45]. Interestingly, AT1R blockers are of common use in clinics and have been proposed for COVID-19 treatment [20]. However, their role in the mechanism of ACE2-mediated SARS-CoV-2 infection remains unclear.

Voltage-gated calcium channels (Ca_V) are a well-known target of GPCRs activity [46]. In particular, $Ca_V2.2$ is a presynaptic subtype highly sensitive to GPCRs that controls synaptic activity [47,48]. Numerous GPCRs, including AT1R and B2R, acutely inhibit $Ca_V2.2$ by different signaling cascades [49,50]. In this regard, we have contributed to characterize the modulation of $Ca_V2.2$ by the growth hormone secretagogue receptor (GHSR) [51–53], the melanocortin 4 receptor (MC4R) [54] and the dopamine 1 receptor (D1R) [55]. On the other hand, growing evidence shows that GPCRs heteromerization can modify the classical GPCR modulation of $Ca_V2.2$ [56–58]. For instance, we have shown that D2R coexpression exacerbates the inhibition of basal $Ca_V2.2$ currents induced by GHSR constitutive activity, and that GHSR coexpression reduces dopamine-evoked acute inhibition of $Ca_V2.2$ currents in presence of D2R [57,58]. Therefore, $Ca_V2.2$ constitute a valuable tool to study changes of GPCRs functionality by interaction with other receptors or membrane proteins, such as ACE2.

Here we explored the role of AT1R and B2R as well as the effect of their ligands on the internalization of GFP-tagged ACE2 (ACE2-GFP) induced by a recombinant RBD of SARS-CoV-2 S protein in a heterologous expression system. Moreover, we monitored changes in AT1R and B2R functionality upon ACE2 coexpression by assaying their effect on $Ca_V2.2$ currents. Our results unmask a role for AT1R and B2R on RBD-induced ACE2 internalization, and provide new insights into the modulation of SARS-CoV-2 infection with an ultimate therapeutic purpose.

2. Results

2.1. RBD induces ACE2-GFP internalization

We first assessed whether RBD induces internalization of ACE2 in our experimental model. We incubated HEK293T cells transfected with ACE2-GFP with recombinant RBD for 40 min and stained the plasma membrane with a live-cell labeling compound previously used by our group [52,53,55]. After the incubation, in RBD-treated cultures a fraction of cells showed clustered GFP signal at the plasma membrane or in intracellular compartments, whereas in vehicle-treated cultures cells only displayed GFP signal uniformly distributed at the plasma membrane (Fig. 1A). Next, we performed an immunostaining against RBD in HEK293T cells expressing ACE2-GFP incubated with RBD for 40 min to assess RBD internalization (Fig. 1B). Consistent with our previous observations, in vehicle-treated cultures we only found cells with GFP signal uniformly distributed at the plasma membrane, whereas in RBD-treated cultures we mostly found cells with GFP signal clustered in spots in the plasma membrane or inside the cell. As expected, red fluorescent signal indicating RBD immunoreactivity was only observed in transfected cells (ACE2-GFP positive) of RBD-treated cultures. Importantly, RBD-immunoreactive signal was distributed in discrete clusters at the plasma membrane and the intracellular compartment and colocalized with GFP signal, suggesting an RBD-ACE2 joint internalization. These observations indicate that RBD induces ACE2-GFP internalization in our experimental system.

2.2. The degree of RBD-induced ACE2-GFP internalization is time-dependent

Next, we estimated ACE2 internalization dynamics by incubating ACE2-GFP-expressing HEK293T cells with vehicle or RBD for 5, 10 and 40 min and assessing the percentage of ACE2-GFP positive cells with different GFP signal patterns (Fig. 2A). Specifically, we grouped cells based on the subcellular distribution of the GFP signal as follows: GFP uniformly distributed in the plasma membrane (PMU GFP), GFP clustered in the plasma membrane (PMC GFP), and GFP clustered in intracellular compartments with or without clustered GFP in the plasma membrane (Internalized GFP). In vehicle-treated cultures, all cells corresponded to the PMU GFP group, whereas in RBD-treated cultures a significant number of cells with PMC GFP or internalized GFP was observed (Fig. 2B). After 5 and 10 min of RBD incubation, the majority of the cells (~65–70%) showed PMC GFP signal, with a small proportion showing internalized GFP at 10 min. Notably, the percentage of cells displaying internalized GFP increased (~60%) and the percentage of cells with PMC GFP (~30%) decreased at 40 min of incubation. In order to statistically compare this observation, we arranged the different GFP signal patterns into degrees of internalization (PMU GFP-degree 0, PMC GFP-degree 1, and Internalized GFP-degree 2) and tested the association between RBD incubation time and the frequency of cells with different ACE2-GFP internalization degree. We found a strong positive association between these two variables ($\chi^2 = 190.03$, $P_{chi} < 0.0001$; Somers' D $= 0.57$, directional coefficient for the association between RBD incubation time and ACE2-GFP internalization degree). These results suggest that RBD induces ACE2 internalization in a time-dependent manner, and allow us to propose that the different patterns of GFP signal discriminated in our system correspond to different degrees of ACE2-GFP internalization.

2.3. AT1R ligands modulate RBD-induced ACE2-GFP internalization

In order to test if AT1R affects RBD-induced ACE2 internalization, we transfected HEK293T cells with ACE2-GFP alone or with ACE2-GFP plus AT1R and incubated them with RBD for 40 min (Fig. 3A). We found that the coexpression of AT1R failed to change the distribution of cells with different GFP signal patterns in both vehicle- and RBD-treated

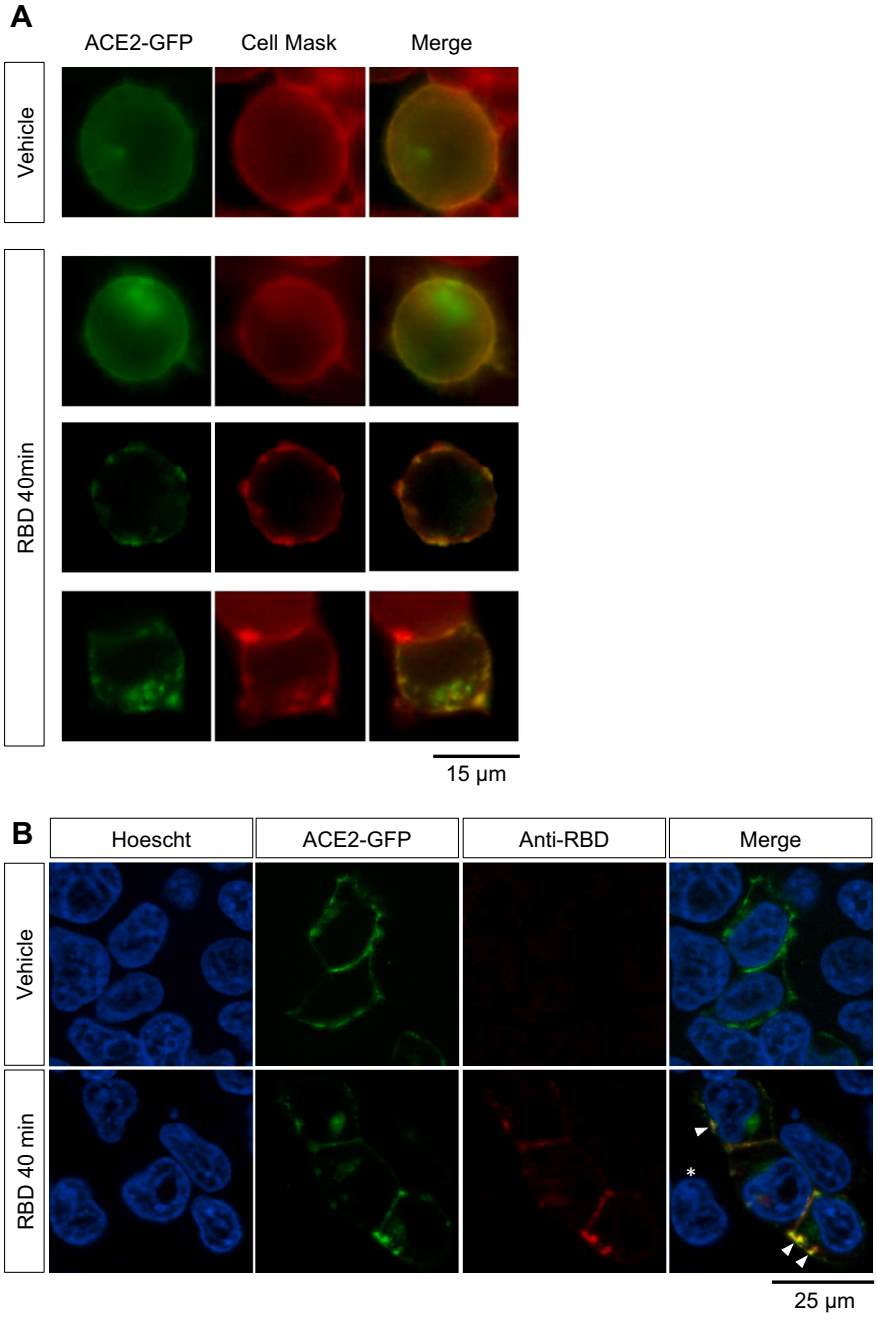

Fig. 1. (A) Example images of the GFP signal patterns identified in cultures of HEK293T cells transfected with ACE2-GFP incubated with vehicle or RBD (10 µg/mL) for 40 min. Objective magnification: 60×. (B) Example images of HEK293T cells transfected with ACE2-GFP incubated with vehicle or RBD 10 µg/mL for 40 min and immunostained against RBD. For nuclei visualization cells were co-stained with Höescht. The asterisk in merged image of RBD-treated cells shows that a non-transfected cell is negative for RBD. Arrowheads point at colocalization of ACE2-GFP and RBD signal. Objective magnification: 63×.

conditions in comparison with cultures only expressing ACE2-GFP. To assess the effect of AT1R ligands on RBD-induced ACE2-GFP internalization, we next incubated cells coexpressing ACE2-GFP and AT1R with vehicle or RBD plus vehicle, an AT1R agonist (Ang II) or an AT1R antagonist (telmisartan) (Fig. 3B). In telmisartan and RBD-coincubated cultures, we found that the percentage of cells with internalized GFP decreased and the percentage of cells with PMC GFP increased in comparison with cultures coincubated with RBD and vehicle. Conversely, the percentage of cells with PMC GFP decreased and the percentage of cells with internalized GFP increased in Ang II and RBD-coincubated cultures in comparison with cultures coincubated with RBD and vehicle. Since AT1R activity is induced by Ang II and reduced by telmisartan [23,59,60], we applied a directional test to evaluate the association between AT1R activation level and ACE2-GFP internalization degree. In particular, we considered AT1R activity levels as 0 in telmisartan-coincubated cells, 1 in vehicle-coincubated cells and 2 in Ang II-coincubated cells, and the internalization degrees as done above (PMU GFP-degree 0, PMC GFP-degree 1, and Internalized GFP-degree 2). We found a significant positive correlation between AT1R activity levels and the frequency of cells displaying the different ACE2-GFP internalization degrees ($\chi^2 = 17.89$, $P_{chi} < 0.01$; Somers' D = 0.24). These data indicate that RBD induced-ACE2 internalization depends on AT1R activity.

2.4. B2R inhibits RBD-induced ACE2-GFP internalization

In order to test if B2R affects RBD-induced ACE2 internalization, we incubated HEK293T cells transfected with ACE2-GFP alone or plus B2R with RBD for 40 min (Fig. 4). In RBD-treated cultures, we found that B2R coexpression dramatically reduced the fraction of cells displaying internalized GFP signal and increased the percentage of cells with PMC GFP signal in comparison with cultures transfected only with ACE2-GFP.

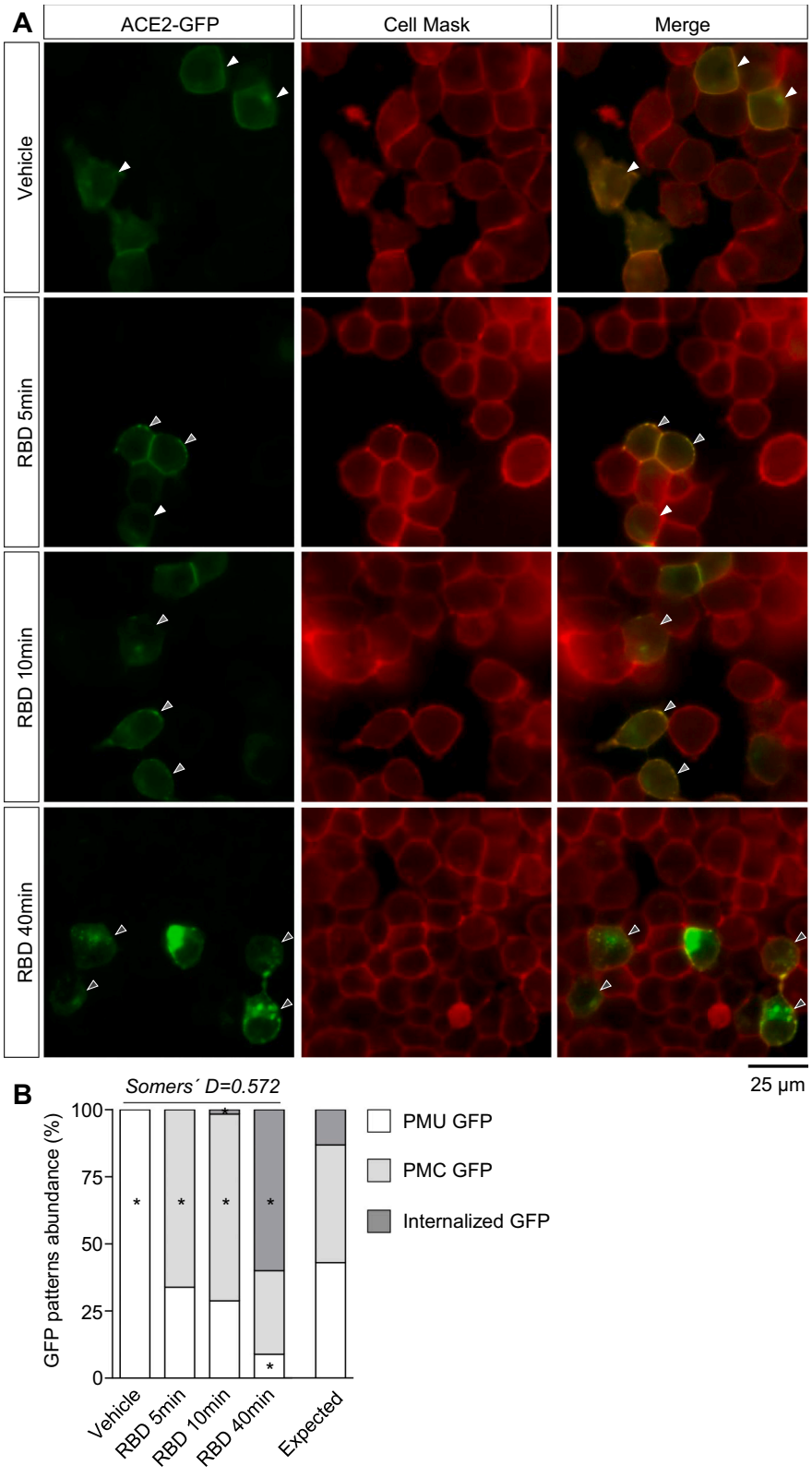

Fig. 2. (A) Representative images of cultures of HEK293T cells transfected with ACE2-GFP incubated with vehicle or RBD (10 µg/mL) for 5, 10 or 40 min. For membrane visualization cells were treated with Cell Mask. Magnification: 60×. Arrowheads indicate the different GFP signal patterns (white: PMU GFP, light gray: PMC GFP and dark gray: internalized GFP). (B) GFP patterns abundance (%) in HEK293T cells transfected with ACE2-GFP upon vehicle or RBD incubation at the specified times. PMU GFP (plasma membrane uniform GFP), PMC GFP (plasma membrane clustered GFP). Association between time of RBD treatment and GFP patterns frequency was evaluated by Chi-square test ($\chi^2 = 190.03$, $P_{chi} < 0.0001$; * indicates different from the expected frequency of the corresponding GFP pattern, $P < P_{corr} = 0.004$; Somers' D = 0.57; n = 45–60 total cells per condition).

Since cells displaying PMC GFP signal may represent an intermediate stage of the ACE2-GFP internalization process, our observations could indicate that B2R delays ACE2 internalization. Additionally, we co-incubated HEK293T cells expressing ACE2-GFP and B2R with RBD and the B2R endogenous ligand bradykinin (BK) for 40 min. In those cultures, we found an increase in the percentage of cells with PMC GFP in comparison with cells coexpressing B2R and ACE2-GFP incubated only with RBD suggesting that BK enhances B2R inhibitory effect on RBD-induced ACE2-GFP internalization.

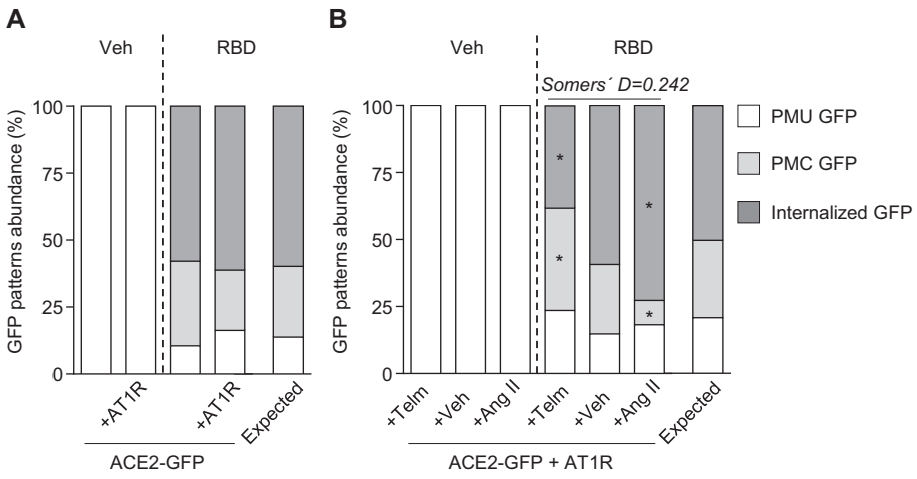

Fig. 3. (A) GFP patterns abundance (%) in cultures of HEK293T cells transfected with ACE2-GFP alone (ACE2-GFP) or co-transfected with AT1R (ACE2-GFP + AT1R) incubated with vehicle or RBD (10 μg/mL) for 40 min. Association between treatments and GFP patterns frequency in RBD-treated groups was evaluated by Chi-square test ($\chi^2 = 1.237$, $P_{chi} = 0.54$; n = 30–50 cells per condition). (B) GFP patterns abundance (%) in cultures of HEK293T cells co-transfected with ACE2-GFP and AT1R (ACE2-GFP + AT1R) co-incubated with vehicle or RBD and vehicle (+Veh), telmisartan (+Telm, 10 μM) or angiotensin II (+Ang II, 1 μM) for 40 min. Telmisartan and Ang II were added to the culture medium 5 min prior to RDB. Association between treatments and GFP patterns frequency in RBD-treated groups was evaluated by Chi-square test ($\chi^2 = 17.89$, $P_{chi} < 0.01$; * indicates different from the expected frequency of the corresponding GFP pattern, $P < P_{corr} = 0.004$; Somers' D = 0.24; n = 35–47 cells per condition).

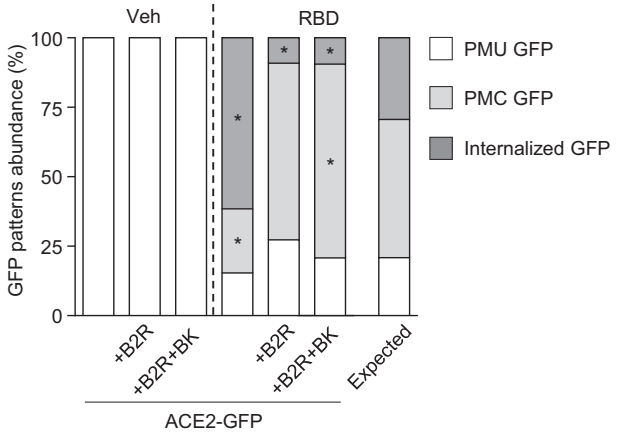

Fig. 4. GFP patterns abundance (%) in cultures of HEK293T cells transfected with ACE2-GFP alone (ACE2) or co-transfected with B2R (+B2R) incubated with vehicle or RBD (10 μg/mL) for 40 min. In +B2R + BK condition, cells were co-incubated with BK plus vehicle or BK plus RBD (BK, 0.5 μM) for 40 min. BK was added to the culture medium 5 min prior to RBD. Association between treatments and GFP patterns frequency in RBD-treated groups was evaluated by Chi-square test ($\chi^2 = 47.29$, $P_{chi} < 0.0001$; * indicates different from the expected frequency of the corresponding GFP pattern, $P < P_{corr} = 0.006$; n = 26–48 cells per condition).

2.5. B2R inhibition of RBD-induced ACE2-GFP internalization persists upon AT1R coexpression but is overcome by Ang II

Increasing evidence indicates that AT1R and B2R form heteromers whose properties differ from the individual receptors [36,43,61,62]. To test if AT1R and B2R coexpression affects RBD-induced ACE2-GFP internalization, we incubated HEK293T cells co-transfected with ACE2-GFP and AT1R or ACE2-GFP, AT1R and B2R with RBD for 40 min (Fig. 5A). We found that the coexpression of B2R reduced the percentage of cells with internalized GFP and increased the percentage of cells with PMC GFP indicating an inhibitory effect of B2R on ACE2-GFP internalization even in presence of AT1R. Afterwards, we assessed whether this action of B2R is modulated by BK or Ang II. To that aim, we co-incubated HEK293T cells expressing ACE2-GFP, AT1R and B2R with vehicle or RBD alone or plus BK or Ang II for 40 min (Fig. 5B). In RBD-treated cultures, BK did not change the frequency of cells with different GFP signal as compared to vehicle-coincubated cultures. However, Ang II induced an increase in the frequency of cells with internalized GFP concomitant with a decrease in the frequency of cells with PMC GFP compared with the other conditions indicating a partial rescue of RBD-induced ACE2-GFP internalization. Taken together, these experiments suggest that Ang II has a pro-internalizing effect that overcomes B2R inhibitory action on RBD-induced ACE2 internalization.

2.6. ACE2-GFP coexpression modifies AT1R-, but not B2R-ligand evoked inhibition of $Ca_V2.2$ currents

Since AT1R and B2R modulated RBD-induced ACE2-GFP internalization, we then explored if conversely ACE2-GFP affects AT1R and B2R ligand-evoked action on $Ca_V2.2$, a well-established GPCRs target [46]. First, we tested the effect of ACE2-GFP coexpression on BK-evoked B2R activity in HEK293T cells expressing $Ca_V2.2$ (plus its auxiliary subunits) and B2R in presence or absence of ACE2-GFP. As shown before [50], BK-evoked B2R activity inhibited $Ca_V2.2$ currents. Similar percentages of $Ca_V2.2$ current inhibition were detected in cells coexpressing ACE2-GFP in presence of BK (Fig. 6A). Interestingly, AT1R co-expression reduced BK-induced $Ca_V2.2$ current inhibition, and such effect was restored to control levels (+ B2R) in cells coexpressing B2R, AT1R and ACE2-GFP. Next, in order to test the effect of ACE2-GFP coexpression on Ang II-evoked AT1R activity we measured calcium currents in HEK293T cells expressing $Ca_V2.2$ (plus its auxiliary subunits) and AT1R in presence or absence of ACE2-GFP. As previously shown [49,57], Ang II-evoked AT1R activity inhibited $Ca_V2.2$ currents (Fig. 6B). Notably, the coexpression of AT1R with either ACE2-GFP, B2R or ACE2-GFP plus B2R decreased Ang II-mediated $Ca_V2.2$ currents inhibition. Thus, ACE2-GFP coexpression impacts on Ang-evoked AT1R action on $Ca_V2.2$ currents but does not affect BK-evoked B2R effect on these currents.

2.7. ACE2-GFP coexpression alters ligand-independent activity of AT1R and B2R on $Ca_V2.2$ currents

To study if ACE2-GFP coexpression modifies the ligand-independent activities of B2R and AT1R, we then assessed $Ca_V2.2$ currents in HEK293T cells expressing B2R, AT1R or both receptors in presence or absence of ACE2-GFP. We found that ACE2-GFP coexpression did not change basal $Ca_V2.2$ macroscopic currents in AT1R-expressing cells but significantly reduced them in B2R-expressing cells, in comparison with cells expressing only the respective GPCR (Fig. 7A and B). Strikingly, ACE2-GFP coexpression increased the $Ca_V2.2$ currents in HEK293T cells expressing B2R and AT1R (Fig. 7C). Thus, ACE2-GFP coexpression has opposite effects on basal $Ca_V2.2$ currents in B2R and B2R-AT1R expressing cells.

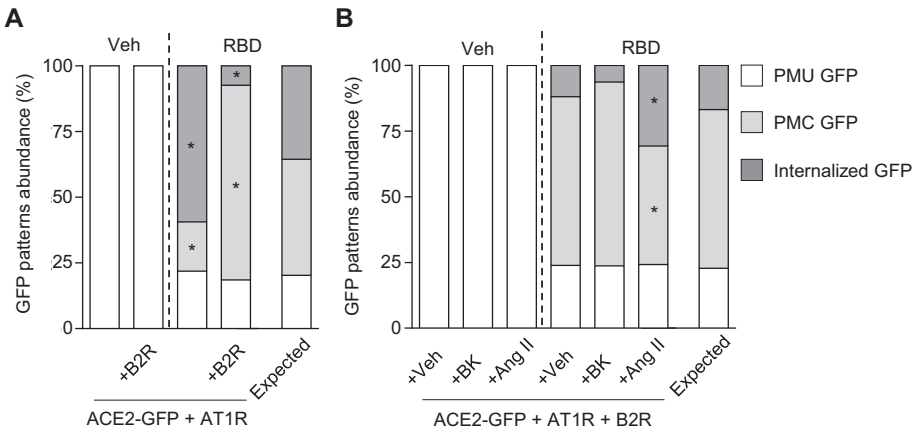

Fig. 5. (A) GFP patterns abundance (%) in cultures of HEK293T cells co-transfected with ACE2-GFP and AT1R (ACE2-GFP + AT1R) or plus B2R (+B2R) incubated with vehicle or RBD (10 μg/mL) for 40 min. Association between treatments and GFP patterns frequency in RBD-treated groups was evaluated by Chi-square test ($\chi^2 = 21.36$, $P_{chi} < 0.0001$; * indicates different from the expected frequency of the corresponding GFP pattern, $P < P_{corr} = 0.008$; n = 28–33 cells per condition). (B) GFP patterns abundance (%) in cultures of HEK293T cells co-transfected with ACE2-GFP, AT1R and B2R (ACE2-GFP + AT1R + B2R) co-incubated with vehicle or RBD (10 μg/mL) and vehicle (+Veh), BK (+BK, 0.5 μM) or angiotensin II (+AngII, 1 μM) for 40 min. For co-incubation, B2R or AT1R agonists were added to the culture medium 5 min prior to RBD. Association between treatments and GFP patterns frequency in RBD-treated groups was evaluated by Chi-square test ($\chi^2 = 14.56$, $P_{chi} < 0.01$; * indicates different from the expected frequency of the corresponding GFP pattern, $P < P_{corr} = 0.006$; n = 33–40 cells per condition).

3. Discussion

ACE2 is a transmembrane enzyme important for the regulation of the RAS that has regained interest because it was recently identified as the receptor for SARS-CoV-2. Thus, the study of the factors and mechanisms that regulate ACE2 internalization would provide new insights into the modulation of coronavirus infection. Here, we not only confirmed that the RBD of SARS-CoV-2 S protein induces ACE2 internalization, but also demonstrated for the first time that this process is modulated by GPCRs involved in the RAS. Using the AT1R agonist Ang II and the AT1R antagonist telmisartan, we revealed that the activity of AT1R positively correlates with the degree of RBD-induced ACE2 internalization. We also uncover a novel and strong inhibitory effect of B2R on RBD-induced ACE2 internalization that persists in the presence of AT1R and is mildly modified by its endogenous ligand BK. Notably, the inhibitory action of B2R coexpression on ACE2 internalization was reversed by Ang II in the presence of AT1R, which positions this hormone as a pro-internalizing factor. Complementary, we found that ACE2 modifies the capability of AT1R and B2R to inhibit $Ca_V2.2$ calcium currents likely due to an interaction with these receptors.

Current results indicate that RBD rapidly induces ACE2-GFP internalization in a time-dependent fashion. ACE2 internalization is induced by SARS-CoV-2 and other related viruses such as HCoV-NL63 and SARS-CoV [7,9,63,64]. RBD is the minimal receptor-binding domain of the S protein from SARS-CoV-2 and its predecessor SARS-CoV, and has been previously used as a model to study viral infections [65]. In cell cultures incubated with RBD, we observed clear signs of ACE2-GFP internalization with cells displaying clustered GFP signal at the cytoplasm or the plasma membrane that colocalized with RBD signal. A similar ACE2 signal pattern denoting internalization has been previously shown by other authors studying SARS-CoV infections. In those reports, nearly all HEK293T cells expressing ACE2-GFP incubated for 3 h with a recombinant RBD, S protein, or lentiviruses pseudotyped with S protein exhibited punctuated cytoplasmic GFP signal [65,66]. However, cells with clustered GFP signal at the plasma membrane (PMC GFP) were not reported presumably due to the longer incubation time tested (3 h) [65,66] in comparison with ours (40 min), which may allow a complete internalization of ACE2. We hypothesize that the prevalence of cells with PMC GFP at short time points indicates an initial stage in the internalization of the ACE2-RBD complex. Further supporting this notion, a similar distribution of clustered signal at the plasma membrane was shown for other membrane proteins endocyted via clathrin-mediated pathways [67] and upon inhibition of membrane receptors internalization [68]. Notably, the kinetics of ACE2-GFP internalization observed in the current study is in agreement with recent observations showing SARS-CoV-2 S protein uptake as early as 5 min, and higher uptake at 30 min of exposure [10].

Here we reveal a novel inhibitory action of B2R on RBD-induced ACE2-GFP internalization. Previous studies have reported effects of B2R retaining receptors at the cell membrane by heteromerization. In this regard, B2R coexpression was shown to delay Ang1–7-induced sequestration of MasR from the plasma membrane [69], and to stabilize B1R at the cell surface in the absence of its ligand [70]. Thus, it is likely that B2R prevents RBD-induced ACE2-GFP internalization due to a direct interaction with ACE2. Further supporting this possibility, we found that ACE2 coexpression alters basal calcium currents in cells expressing B2R alone or plus AT1R. Besides, the formation of complexes between ACE2 and other receptors of the RAS (AT1R, AT2R, MasR) has been extensively demonstrated [21,22,69]. Interestingly, we also observed that neither AT1R coexpression, a GPCR known to heteromerize with B2R [43,61,62], nor BK application were able to unlock the B2R inhibition of ACE2 internalization suggesting that the functional crosstalk between B2R and ACE2 is strong. In the context of SARS-CoV-2 infection, our findings indicate that B2R is a protective factor that acts interrupting or delaying viral entry. Further protective effects of B2R might emerge from the retention of ACE2 on the plasma membrane that could avoid Ang II accumulation and promote the Ang 1–7/MasR axis counteracting Ang II detrimental effects in the infection and inflammation [16].

We found that RBD-induced ACE2-GFP internalization is modulated by AT1R. Previous studies have shown that Ang II triggers AT1R and ACE2 co-internalization [22], and ACE2 coexpression downregulates Ang II induced-AT1R signaling [21] as a consequence of an interaction between ACE2 and AT1R. Further supporting this, in our electrophysiological experiments ACE2 coexpression dramatically impaired Ang II-induced AT1R inhibitory action on $Ca_V2.2$ calcium currents. Thus, it is likely that Ang II enhances ACE2 internalization trough the AT1R-ACE2 complex increasing the percentage of cells with internalized ACE2-GFP. Conversely, telmisartan binding to AT1R would modify the conformation of the ACE2-AT1R complex and prevent the interaction of RBD with ACE2 leading to a reduction in the percentage of cells with internalized ACE2-GFP. Interestingly, Ang II not only increased ACE2-GPF internalization in presence of AT1R, but also in cells coexpressing AT1R and B2R, unlocking the strong B2R inhibition of RBD-induced ACE2 internalization. This observation indicates a stronger influence of AT1R on ACE2 than B2R. In summary, our findings show that Ang II is a potent pro-internalizing factor that might promote SARS-CoV-2 entry, while telmisartan has opposite effects and might act as an infection delaying

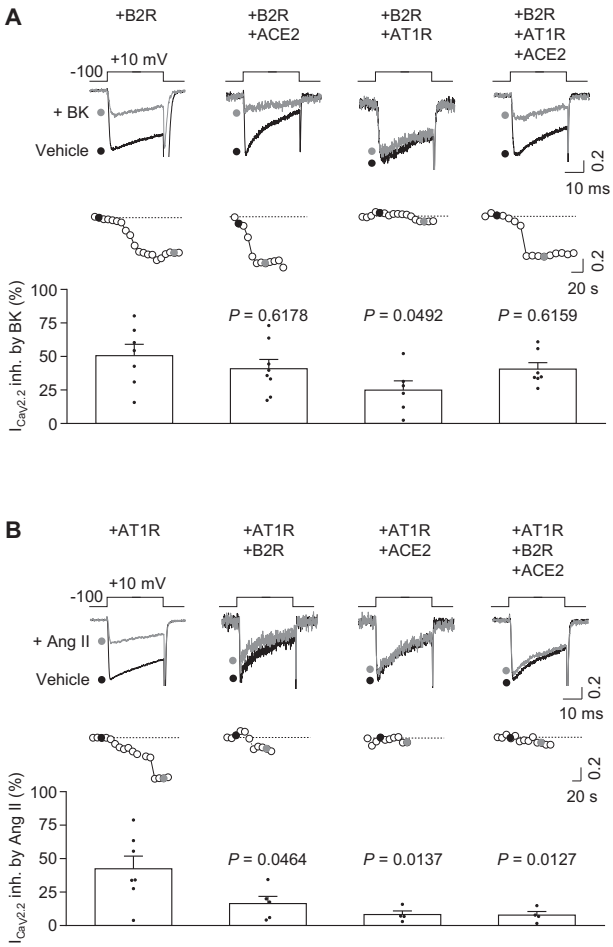

Fig. 6. (A) Representative traces (top) of $Ca_V2.2$ calcium currents ($I_{CaV2.2}$) and time courses (middle) of HEK293T cells co-transfected with $Ca_V2.2$ and B2R (+B2R, $n = 7$), or $Ca_V2.2$, B2R and ACE2 (+B2R + ACE2, $n = 8$), or $Ca_V2.2$, B2R and AT1R (+B2R + AT1R, $n = 6$), or $Ca_V2.2$, B2R, AT1R and ACE2 (+B2R + AT1R + ACE2, n = 7) in control condition (vehicle) and 0.5 μM BK application (+BK); 0.1 ACE2-GFP or GPCR: $Ca_V2.2$ molar ratio. Black and gray dots correspond to vehicle and BK traces respectively. Bars (bottom) represent the average $I_{CaV2.2}$ inhibition by BK application for each condition. One Way ANOVA and Tukey's post-test (*P* value estimated versus +B2R). (B) Representative traces (top) of $Ca_V2.2$ calcium current ($I_{CaV2.2}$) and time courses (middle) of HEK293T cells co-transfected with $Ca_V2.2$, and AT1R (+AT1R, n = 7), or $Ca_V2.2$, AT1R and B2R (+AT1R + B2R, $n = 5$), or $Ca_V2.2$, AT1R and ACE2 (+AT1R + ACE2, $n = 4$), or $Ca_V2.2$, AT1R, B2R and ACE2 (+B2R + AT1R + ACE2, n = 4) in control condition (vehicle) and 1 μM Ang II application (+Ang II); 0.1 ACE2-GFP or GPCR: $Ca_V2.2$ molar ratio. Black and gray dots correspond to vehicle and Ang II traces respectively. Bars (bottom) represent the average $I_{CaV2.2}$ inhibition by angiotensin II application for each condition. One Way ANOVA and Tukey's post-test (P value estimated versus +AT1R).

agent. This uncovers the importance of AT1R as a druggable target for the management of COVID-19.

Acute respiratory distress syndrome is a hallmark of severe cases of COVID-19 and is the result of a systemic inflammatory response known as the cytokine storm [71]. It has been suggested that accumulation of Ang II due to the reduction in plasma membrane ACE2 during SARS-CoV-2 infection contributes to such pro-inflammatory state [1,13,18]. AT1R blockers have been proposed to avoid the detrimental effects of Ang II accumulation [19,20]. In this regard, in a recent clinical trial in COVID-19 patients telmisartan showed potent anti-inflammatory actions as well as a reduction in the morbidity and mortality of the disease [72]. The modulation of RBD-induced ACE2 internalization by AT1R ligands described here demonstrates an effect of these compounds in the infection *per se*, besides the previously shown in the inflammatory state of patients suffering from COVID-19. This suggests a dual role of AT1R ligands in the disease: Ang II might act as a pro-inflammatory and pro-internalizing factor, whereas telmisartan might act as an anti-inflammatory and an infection-delaying agent. The pro-internalizing action of Ang II found here extends the knowledge about the mechanisms underlying the occurrence of hypertension as a risk factor for the severity of COVID-19 [28–30,73]. On the other hand, the anti-internalizing action of telmisartan supports the use of AT1R blockers to avoid or counteract Ang II detrimental effects and could explain in part the reduced severity and mortality of the disease in hypertensive patients chronically treated with AT1R [74–76].

4. Conclusions

In summary, our study demonstrates that AT1R and B2R modulate the internalization of ACE2 induced by a SARS-CoV-2 surface protein, and inversely, ACE2 modifies AT1R and B2R functionality. Altogether, the current findings contribute to understand the role of RAS components in the susceptibility to SARS-CoV-2 infection and in the severity of COVID-19, and pave the way through the development of drugs aimed to limit infections caused by viruses using ACE2 as membrane receptor.

5. Materials and methods

5.1. Human Embryonic Kidney 293T (HEK293T) cell culture

HEK293T cells were grown in Dulbecco's modified Eagle's medium (DMEM; Gibco) with 10% fetal bovine serum (FBS; Internegocios). At 80% confluence cells were detached with citric saline solution (0.135 M KCl, 0.015 M sodium citrate) and plated in a 24-well plate for electrophysiology assays, in 35 mm dishes for live imaging assays, and in 12 mm glasses for immunofluorescence experiments.

5.2. HEK293T cells transfection

Transfections were done using Lipofectamine 2000 (Invitrogen) and Opti-MEM (Gibco). Lipofectamine was used according to the manufacturer's specifications in a ratio of 2.5 μL lipofectamine/1.25 μg of total DNA.

For imaging experiments cells were transfected with plasmids containing ACE2-GFP (donated by Dr. Eric Lazartigues) with or without plasmids containing AT1R or B2R (both donated by Dr. Mark Shapiro, University of Texas Health, San Antonio, TX, USA) in the combination required for each experimental condition. For electrophysiology experiments cells were transfected with plasmids containing Ca_V subunit $Ca_V2.2$ (#AF055477), and plasmids bearing the auxiliary subunits $Ca_V\beta_3$ (#M88751) and $Ca_V\alpha_2\delta_1$ (#AF286488) (all Ca_V subunits were generously provided by Dr. D. Lipscombe, Brown University, Providence, RI, USA) with or without plasmids containing AT1R, B2R or ACE2-GFP as it corresponded to the experimental condition. To identify transfected cells in electrophysiology experiments, 0.2 μg of an eGFP (enhanced green fluorescent protein)-containing plasmid was used. In all transfections experiments an empty plasmid (pcDNA3.1 (+)) was co-transfected when needed to maintain an equal amount of total cDNA throughout conditions. Transfected cells were cultured for 24 h prior to the experiment beginning to allow plasmid expression.

5.3. Drugs

The RBD of spike protein 1 from SARS-CoV-2 was synthesized as described before [77]. Angiotensin II was purchased from Sigma-Aldrich (A9525). Bradykinin was acquired from Alomene Labs (GPB-200). Telmisartan, acquired from Rundu Pharma, was donated by Dr. Valeria Martínez (Centro de Química Inorgánica (CEQUINOR), Facultad de Ciencias Exactas, Universidad Nacional de La Plata, La Plata, Argentina).

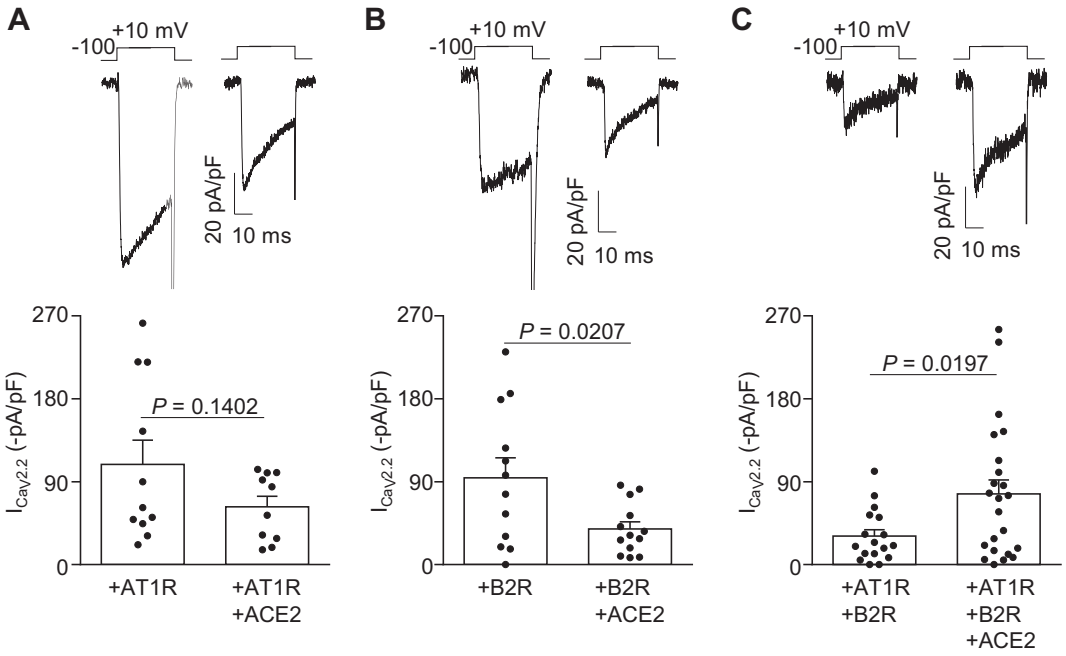

Fig. 7. Representative traces (top) of $Ca_V2.2$ calcium currents ($I_{CaV2.2}$) from HEK293T cells co-transfected with (A) $Ca_V2.2$ and AT1R (+AT1R, $n = 11$) or $Ca_V2.2$, AT1R and ACE2-GFP (+AT1R + ACE2, $n = 10$), (B) $Ca_V2.2$ and B2R (+B2R, $n = 12$) or $Ca_V2.2$, B2R and ACE2-GFP (+B2R + ACE2, $n = 13$), and (C) $Ca_V2.2$, B2R and AT1R (+AT1R + B2R, $n = 17$) or $Ca_V2.2$, B2R, AT1R and ACE2-GFP (+B2R + AT1R + ACE2, $n = 23$); 0.1 ACE2-GFP: or GPCR: $Ca_V2.2$ molar ratio. Bars (bottom) represent the average $I_{CaV2.2}$ for each condition. Unpaired Student's *t*-test.

5.4. Live imaging

HEK293T cells transfected with ACE2-GFP alone or plus the corresponding plasmids (AT1R, B2R or both) were incubated with vehicle or RBD (10 μg/mL) for the time specified in the Results section. In co-incubation experiments cells were incubated with AT1R or BK ligands (telmisartan [10 μM], Ang II [1 μM], and BK [0.5 μM]) and vehicle or RBD for 40 min. The ligands were added to the culture medium 5 min prior to vehicle or RBD. For live imaging experiments, cells were washed with phosphate buffered-saline (PBS, pH = 7.4) and incubated for 1 min with Cell Mask solution (ThermoFisher, 1:2000 in DMEM) for membrane visualization. Afterwards, cells were washed with PBS and covered with a 22 mm squared glass. Fluorescent images were acquired with a 60×/0.80 objective using a Nikon Eclipse 50i and a DS-Ri1 Nikon digital camera with a 0.55× adapter in the green and red channel. All images were taken under the same optical and light conditions. Image visualization and edition was made with the open-source software Fiji [78].

5.5. Immunofluorescence

HEK293T cells transfected with ACE2-GFP and incubated with vehicle or RBD (10 μg/mL) for 40 min were washed with PBS and fixed with 4% paraformaldehyde in PBS for 30 min. After removal of the fixative solution, cells were washed with PBS and incubated with normal donkey serum (0.3%) diluted in PBS with Triton-X (0.25%) for 1 h. Afterwards, cells were incubated with a rabbit polyclonal anti-SARS-CoV-2 spike protein (receptor binding domain (RBD) of spike 1, GeneTex, cat. GTX135385, 1:500) for 24 h at room temperature. Finally, cells were washed with PBS, incubated with an AlexaFluor 594-conjugated anti-rabbit antibody (Invitrogen, cat. A11008, 1:500) for 2 h and mounted on glass slides with mounting media. Fluorescent images were acquired with a Zeiss AxioObserver D1 equipped with an Apotome.2 structured illumination module and an AxioCam 506 monochrome camera. Image visualization and edition was made with the open-source software Fiji [78].

5.6. Electrophysiology

On the experimental day, cells were detached from the culture plate with 0.25 mg/mL trypsin (Microvet), rinsed twice and kept at room temperature (~24 °C) in DMEM. Patch-clamp experiments in whole-cell and voltage-clamp configuration were performed using Axopatch 200 amplifier (Molecular Devices). Data were sampled at 20 kHz and filtered at 10 kHz (−3 dB) using PCLAMP8.2.0.235 software (Molecular Devices). Recording pipettes with a resistance between 2 and 4 MΩ were used and filled with internal solution (in mM): 134 CsCl, 10 EGTA, 1 EDTA, 10 HEPES and 4 MgATP (pH 7.2 with CsOH). Series resistances of <6 MΩ were admitted and compensated 80% with a 10 μs lag time. Cells with a leak current higher than 100 pA at −100 mV were discarded and leak current was subtracted online using a P/−4 protocol. Solutions were perfused from a 10 mL syringe containing bath solution placed 30 cm over the patch clamp chamber so the gravity drives the liquid to the chamber. A solution containing angiotensin II or bradykinin was applied with this system connected to different ports of the stopcocks. The external calcium solution (2 mM) contained (in mM): 140 choline chloride, 10 HEPES, 1 $MgCl_2{\cdot}6H_2O$ and $2CaCl_2{\cdot}2H_2O$ (pH 7.3–7.4 with CsOH). The test-pulse protocol consisted in square pulses applied from −100 to +10 mV for 30 ms every 10 s All recordings were obtained at room temperature (~24 °C).

5.7. Statistics

Data of GFP patterns abundance from imaging experiments were represented in Graph Pad Prism (GraphPad Software, Inc.) and analyzed in IBM SPSS Statistics 26 (IBM Corp., Armonk, N.Y., SA). For the analysis, data were distributed in contingency tables and analyzed by the Chi-square (χ^2) test to determine the association between variables. The association was considered statistically significant when the P corresponding to the χ^2 value (P_{chi}) was lower than 0.05. To determine the statistical significance of the difference between the observed and expected frequencies of GFP patterns abundance in each condition, an adjusted standardized residual (z-score) was calculated for each cell of

the contingency table and transformed into a *P* value. The abundance of a GFP pattern was considered statistically different from the expected frequency when its calculated *P* value was lower than the P corrected for type I error (P_{corr}) [79,80], and was indicated with an asterisk in the graph. The expected GFP pattern frequencies were displayed in the corresponding graph. In cases with a significant association between two ordinal variables, the Somers' D coefficient was used to determine the direction of the association (positive or negative). The Somers' D coefficient takes values from −1 to 1. The sign of the coefficient indicates the direction of the association, and the absolute value the strength, being 0 the lowest and 1 the highest.

Electrophysiology data were analyzed and visualized using the GraphPad Prism 6 (GraphPad Software, Inc.) and OriginPro 9 (OriginLab) software. *P* values were calculated from unpaired Student's *t*-tests (normally distributed data), and multiple comparison One Way ANOVA with Tukey's post-test (normally distributed data). The specific statistical test used was indicated for each data set in the corresponding figure. Data were expressed as mean ± standard error of the mean (SEM).

CRediT authorship contribution statement

Andrea Estefanía Portales: Formal analysis, Investigation, Visualization, Writing – original draft, Writing – review & editing, Data curation. **Emilio Román Mustafá:** Investigation, Formal analysis, Visualization, Writing – review & editing. **Clara Inés McCarthy:** Writing – review & editing. **María Paula Cornejo:** Investigation, Writing – review & editing. **Paula Monserrat Couto:** Resources. **Mariela Mercedes Gironacci:** Resources, Writing – review & editing. **Julio Javier Caramelo:** Resources. **Mario Perelló:** Resources, Writing – review & editing. **Jesica Raingo:** Conceptualization, Supervision, Project administration, Funding acquisition, Writing – review & editing, Data curation.

Declaration of competing interest

The authors declare that there are no conflicts of interest.

Data availability

Data will be made available on request.

Acknowledgments

We thank the Profesional de Apoyo Principal Dr. Silvia Susana Rodriguez (Comisión de Investigaciones Científicas, Provincia de Buenos Aires CIC-PBA) for her excellent technical work.

Funding

This work was supported by grants from the Fondo para la Investigación Científica y Tecnológica (FONCyT, PICT2017-0602 to J.R. and PICT2016-1084 to M.P.).

References

[1] T. C, B. S, B. WC, Angiotensin-converting enzyme 2 is a key modulator of the renin-angiotensin system in cardiovascular and renal disease, Curr. Opin. Nephrol. Hypertens. 20 (2011) 62–68, https://doi.org/10.1097/MNH.0B013E328341164A.

[2] X. P, S. S, L. E, ACE2/ANG-(1-7)/Mas pathway in the brain: the axis of good, Am. J. Physiol. Regul. Integr. Comp. Physiol. 300 (2011), https://doi.org/10.1152/AJPREGU.00222.2010.

[3] M.P. Ocaranza, J.A. Riquelme, L. García, J.E. Jalil, M. Chiong, R.A.S. Santos, S. Lavandero, Counter-regulatory renin–angiotensin system in cardiovascular disease, Nat. Rev. Cardiol. 172 (2019) 116–129, https://doi.org/10.1038/s41569-019-0244-8, 17 (2019).

[4] R.A.S. Santos, A.C.S. e Silva, C. Maric, D.M.R. Silva, R.P. Machado, I. de Buhr, S. Heringer-Walther, S.V.B. Pinheiro, M.T. Lopes, M. Bader, E.P. Mendes, V. S. Lemos, M.J. Campagnole-Santos, H.-P. Schultheiss, R. Speth, T. Walther, Angiotensin-(1–7) is an endogenous ligand for the G protein-coupled receptor Mas, Proc. Natl. Acad. Sci. 100 (2003) 8258–8263, https://doi.org/10.1073/PNAS.1432869100.

[5] M. Letko, A. Marzi, V. Munster, Functional assessment of cell entry and receptor usage for SARS-CoV-2 and other lineage B betacoronaviruses, Nat. Microbiol. 54 (2020) 562–569, https://doi.org/10.1038/s41564-020-0688-y, 5 (2020).

[6] Y. Wan, J. Shang, R. Graham, R.S. Baric, F. Li, Receptor recognition by the novel coronavirus from Wuhan: an analysis based on decade-long structural studies of SARS coronavirus, J. Virol. 94 (2020) 127–147.

[7] H. M, K.-W. H, S. S, K. N, H. T, E. S, S. TS, H. G, W. NH, N. A, M. MA, D. C, P. S, SARS-CoV-2 cell entry depends on ACE2 and TMPRSS2 and is blocked by a clinically proven protease inhibitor, Cell 181 (2020) 271–280, e8, https://doi.org/10.1016/J.CELL.2020.02.052.

[8] E. Barrow, A.V. Nicola, J. Liu, Multiscale perspectives of virus entry via endocytosis, Virol. J. 101 (2013) 1–11, https://doi.org/10.1186/1743-422X-10-177, 10 (2013).

[9] R. Lu, X. Zhao, J. Li, P. Niu, B. Yang, H. Wu, W. Wang, H. Song, B. Huang, N. Zhu, Y. Bi, X. Ma, F. Zhan, L. Wang, T. Hu, H. Zhou, Z. Hu, W. Zhou, L. Zhao, J. Chen, Y. Meng, J. Wang, Y. Lin, J. Yuan, Z. Xie, J. Ma, W.J. Liu, D. Wang, W. Xu, E. C. Holmes, G.F. Gao, G. Wu, W. Chen, W. Shi, W. Tan, Genomic characterisation and epidemiology of 2019 novel coronavirus: implications for virus origins and receptor binding, Lancet. 395 (2020) 565–574, https://doi.org/10.1016/S0140-6736(20)30251-8.

[10] A. Bayati, R. Kumar, V. Francis, P.S. McPherson, SARS-CoV-2 infects cells after viral entry via clathrin-mediated endocytosis, J. Biol. Chem. 296 (2021) 100306, https://doi.org/10.1016/j.jbc.2021.100306.

[11] O. X, L. Y, L. X, L. P, M. D, R. L, G. L, G. R, C. T, H. J, X. Z, M. Z, C. X, C. J, H. K, J. Q, W. J, Q. Z, Characterization of spike glycoprotein of SARS-CoV-2 on virus entry and its immune cross-reactivity with SARS-CoV, Nat. Commun. 11 (2020), https://doi.org/10.1038/S41467-020-15562-9.

[12] G. I, B. S, H. P, P. S, S. I, M. MO, S. G, H. H, K. T, W. F, E. J, D. C, P. S, Differential downregulation of ACE2 by the spike proteins of severe acute respiratory syndrome coronavirus and human coronavirus NL63, J. Virol. 84 (2010) 1198–1205, https://doi.org/10.1128/JVI.01248-09.

[13] Y. Liu, Y. Yang, C. Zhang, F. Huang, F. Wang, J. Yuan, Z. Wang, J. Li, J. Li, C. Feng, Z. Zhang, L. Wang, L. Peng, L. Chen, Y. Qin, D. Zhao, S. Tan, L. Yin, J. Xu, C. Zhou, C. Jiang, L. Liu, Clinical and biochemical indexes from 2019-nCoV infected patients linked to viral loads and lung injury 63 (2020) 364–374, https://doi.org/10.1007/s11427-020-1643-8.

[14] Y. Imai, K. Kuba, S. Rao, Y. Huan, F. Guo, B. Guan, P. Yang, R. Sarao, T. Wada, H. Leong-Poi, M.A. Crackower, A. Fukamizu, C.-C. Hui, L. Hein, S. Uhlig, A. S. Slutsky, C. Jiang, J.M. Penninger, Angiotensin-converting enzyme 2 protects from severe acute lung failure, Nat. 4367047 (2005) 112–116, https://doi.org/10.1038/nature03712, 436 (2005).

[15] K. Kuba, Y. Imai, S. Rao, H. Gao, F. Guo, B. Guan, Y. Huan, P. Yang, Y. Zhang, W. Deng, L. Bao, B. Zhang, G. Liu, Z. Wang, M. Chappell, Y. Liu, D. Zheng, A. Leibbrandt, T. Wada, A.S. Slutsky, D. Liu, C. Qin, C. Jiang, J.M. Penninger, A crucial role of angiotensin converting enzyme 2 (ACE2) in SARS coronavirus–induced lung injury, Nat. Med. 118 (2005) 875–879, https://doi.org/10.1038/nm1267, 11 (2005).

[16] L. Samavati, B.D. Uhal, ACE2, much more than just a receptor for SARS-COV-2, Front. Cell. Infect. Microbiol. 10 (2020) 317, https://doi.org/10.3389/FCIMB.2020.00317.

[17] M.A. Matthay, L.B. Ware, G.A. Zimmerman, The acute respiratory distress syndrome, J. Clin. Invest. 122 (2012) 2731–2740, https://doi.org/10.1172/JCI60331.

[18] V.G. Cardoso, G.L. Gonçalves, J.M. Costa-Pessoa, K. Thieme, B.B. Lins, F.A. M. Casare, M.C. de Ponte, N.O.S. Camara, M. Oliveira-Souza, Angiotensin II-induced podocyte apoptosis is mediated by endoplasmic reticulum stress/PKC-δ/p38 MAPK pathway activation and trough increased Na+/H+ exchanger isoform 1 activity, BMC Nephrol. 191 (2018) 1–12, https://doi.org/10.1186/S12882-018-0968-4, 19 (2018).

[19] R.P. Rothlin, H.M. Vetulli, M. Duarte, F.G. Pelorosso, Telmisartan as tentative angiotensin receptor blocker therapeutic for COVID-19, Drug Dev. Res. 81 (2020) 768–770, https://doi.org/10.1002/ddr.21679.

[20] D. Gurwitz, Angiotensin receptor blockers as tentative SARS-CoV-2 therapeutics, Drug Dev. Res. 81 (2020) 537–540, https://doi.org/10.1002/ddr.21656.

[21] R. Franco, A. Lillo, R. Rivas-Santisteban, A.I. Rodríguez-Pérez, I. Reyes-Resina, J. L. Labandeira-García, G. Navarro, Functional complexes of angiotensin-converting enzyme 2 and renin-angiotensin system receptors: expression in adult but not fetal lung tissue, Int. J. Mol. Sci. 21 (2020) 9602, 21 (2020) 9602, https://doi.org/10.3390/IJMS21249602.

[22] M.R. Deshotels, H. Xia, S. Sriramula, E. Lazartigues, C.M. Filipeanu, Angiotensin II mediates angiotensin converting enzyme type 2 internalization and degradation through an angiotensin II type I receptor-dependent mechanism, Hypertension. 64 (2014) 1368–1375, https://doi.org/10.1161/HYPERTENSIONAHA.114.03743.

[23] T. Takezako, H. Unal, S.S. Karnik, K. Node, Current topics in angiotensin II type 1 receptor research: focus on inverse agonism, receptor dimerization and biased agonism, Pharmacol. Res. 123 (2017) 40, https://doi.org/10.1016/J.PHRS.2017.06.013.

[24] E. Braun-Menendez, J.C. Fasciolo, L.F. Leloir, J.M. Muñoz, The substance causing renal hypertension, J. Physiol. 98 (1940) 283, https://doi.org/10.1113/JPHYSIOL.1940.SP003850.

[25] F. ML, H. H, S. W, W. G, M. P, E. P, S. KG, H. A, M.-E. W, H. J, Autoantibodies against the angiotensin receptor (AT1) in patients with hypertension, J. Hypertens. 18 (2000) 945–953, https://doi.org/10.1097/00004872-200018070-00017.

[26] W. G, S. I, Agonistic autoantibodies directed against G-protein-coupled receptors and their relationship to cardiovascular diseases, Semin. Immunopathol. 36 (2014) 351–363, https://doi.org/10.1007/S00281-014-0425-9.

[27] C.N. Young, R.L. Davisson, Angiotensin-II, the brain, and hypertension, Hypertension. 66 (2015) 920–926, https://doi.org/10.1161/HYPERTENSIONAHA.115.03624.

[28] J. Yang, Y. Zheng, X. Gou, K. Pu, Z. Chen, Q. Guo, R. Ji, H. Wang, Y. Wang, Y. Zhou, Prevalence of comorbidities and its effects in patients infected with SARS-CoV-2: a systematic review and meta-analysis, Int. J. Infect. Dis. 94 (2020) 91–95, https://doi.org/10.1016/J.IJID.2020.03.017.

[29] J. Zhang, J. Wu, X. Sun, H. Xue, J. Shao, W. Cai, Y. Jing, M. Yue, C. Dong, Association of hypertension with the severity and fatality of SARS-CoV-2 infection: a meta-analysis, Epidemiol. Infect. 148 (2020) (doi:10.1017/S095026882000117X).

[30] F. Zhou, T. Yu, R. Du, G. Fan, Y. Liu, Z. Liu, J. Xiang, Y. Wang, B. Song, X. Gu, L. Guan, Y. Wei, H. Li, X. Wu, J. Xu, S. Tu, Y. Zhang, H. Chen, B. Cao, Clinical course and risk factors for mortality of adult inpatients with COVID-19 in Wuhan, China: a retrospective cohort study, Lancet. 395 (2020) 1054–1062, https://doi.org/10.1016/S0140-6736(20)30566-3.

[31] D. Wang, B. Hu, C. Hu, F. Zhu, X. Liu, J. Zhang, B. Wang, H. Xiang, Z. Cheng, Y. Xiong, Y. Zhao, Y. Li, X. Wang, Z. Peng, Clinical characteristics of 138 hospitalized patients with 2019 novel coronavirus–infected pneumonia in Wuhan, China, JAMA. 323 (2020) 1061–1069, https://doi.org/10.1001/JAMA.2020.1585.

[32] G. Grasselli, A. Zangrillo, A. Zanella, M. Antonelli, L. Cabrini, A. Castelli, D. Cereda, A. Coluccello, G. Foti, R. Fumagalli, G. Iotti, N. Latronico, L. Lorini, S. Merler, G. Natalini, A. Piatti, M.V. Ranieri, A.M. Scandroglio, E. Storti, M. Cecconi, A. Pesenti, C.-19 L.I. Network, E. Agosteo, V. Alaimo, G. Albano, A. Albertin, A. Alborghetti, G. Aldegheri, B. Antonini, E. Barbara, N. Belgiorno, M. Belliato, A. Benini, E. Beretta, L. Bianciardi, S. Bonazzi, M. Borelli, E. Boselli, N. Bronzini, C. Capra, L. Carnevale, G. Casella, G. Castelli, E. Catena, S. Cattaneo, D. Chiumello, S. Cirri, G. Citerio, S. Colombo, D. Coppini, A. Corona, P. Cortellazzi, E. Costantini, R.D. Covello, G. De Filippi, M.D. Poli, F. Della Mura, G. Evasi, R. Fernandez-Olmos, A.F. Molinari, M. Galletti, G. Gallioli, M. Gemma, P. Gnesin, L. Grazioli, S. Greco, P. Gritti, P. Grosso, L. Guatteri, D. Guzzon, F. Harizay, R. Keim, G. Landoni, T. Langer, A. Lombardo, A. Malara, E. Malpetti, F. Marino, G. Marino, M. G. Mazzoni, G. Merli, A. Micucci, F. Mojoli, S. Muttini, A. Nailescu, M. Panigada, P. Perazzo, G.B. Perego, N. Petrucci, A. Pezzi, A. Protti, D. Radrizzani, M. Raimondi, M. Ranucci, F. Rasulo, M. Riccio, R. Rona, C. Roscitano, P. Ruggeri, A. Sala, G. Sala, L. Salvi, P. Sebastiano, P. Severgnini, I. Sforzini, F.D. Sigurtà, M. Subert, P. Tagliabue, C. Troiano, R. Valsecchi, U. Viola, G. Vitale, M. Zambon, E. Zoia, Baseline characteristics and outcomes of 1591 patients infected with SARS-CoV-2 admitted to ICUs of the Lombardy Region, Italy, JAMA 323 (2020) 1574–1581, https://doi.org/10.1001/JAMA.2020.5394.

[33] O. BO, L. E, F. CM, Angiotensin type 1 receptor-dependent internalization of SARS-CoV-2 by angiotensin-converting enzyme 2, Hypertens. (Dallas, Tex. 1979) 77 (2021) E42–E43, https://doi.org/10.1161/HYPERTENSIONAHA.120.16795.

[34] K.K.V. Haack, N.A. McCarty, Functional consequences of GPCR heterodimerization: GPCRs as allosteric modulators, Pharm. 4 (2011) 509–523, 4 (2011) 509–523, https://doi.org/10.3390/PH4030509.

[35] B. K, J.-T. J, D. D, C. PBS, H. TE, Exploring functional consequences of GPCR oligomerization requires a different lens, Prog. Mol. Biol. Transl. Sci. 169 (2020) 181–211, https://doi.org/10.1016/BS.PMBTS.2019.11.001.

[36] R.M. NL, S. MG, P. AM, G. MM, Angiotensin receptors heterodimerization and trafficking: how much do they influence their biological function? Front. Pharmacol. 11 (2020) https://doi.org/10.3389/FPHAR.2020.01179.

[37] S. R, H. TE, The dynamics of GPCR oligomerization and their functional consequences, Int. Rev. Cell Mol. Biol. 338 (2018) 141–171, https://doi.org/10.1016/BS.IRCMB.2018.02.005.

[38] D. Regoli, J. Barabé, W.K. Park, Receptors for Bradykinin in Rabbit Aortae, Doi: 10.1139/Y77-115 55, 2011, pp. 855–867, https://doi.org/10.1139/Y77-115.

[39] M. Rocha E Silva, W.T. Beraldo, G. Rosenfeld, Bradykinin, a hypotensive and smooth muscle stimulating factor released from plasma globulin by snake venoms and by trypsin, Am. J. Physiol. 156 (1949) 261–273, https://doi.org/10.1152/AJPLEGACY.1949.156.2.261.

[40] Q. U, A. S, Vasopressor meets vasodepressor: the AT1-B2 receptor heterodimer, Biochem. Pharmacol. 88 (2014) 284–290, https://doi.org/10.1016/J.BCP.2014.01.019.

[41] C. GS, M. AC, J. MT, A. EH, C. TJ, T. AP, F. DC, B.-C. ML, L. FR, T. RC, F. ZB, C. RP, T. RM, C. MH, An interaction of renin-angiotensin and kallikrein-kinin systems contributes to vascular hypertrophy in angiotensin II-induced hypertension: in vivo and in vitro studies, PLoS One 9 (2014), https://doi.org/10.1371/JOURNAL.PONE.0111117.

[42] P.C. Wilson, M.H. Lee, K.M. Appleton, H.M. El-Shewy, T.A. Morinelli, Y. K. Peterson, L.M. Luttrell, A.A. Jaffa, The arrestin-selective angiotensin AT1 receptor agonist [Sar1,Ile4,Ile8]-AngII negatively regulates bradykinin B2 receptor signaling via AT1-B2 receptor heterodimers, J. Biol. Chem. 288 (2013) 18872–18884, https://doi.org/10.1074/JBC.M113.472381.

[43] U. Quitterer, A. Pohl, A. Langer, S. Koller, S. AbdAlla, A cleavable signal peptide enhances cell surface delivery and heterodimerization of Cerulean-tagged angiotensin II AT1 and bradykinin B2 receptor, Biochem. Biophys. Res. Commun. 409 (2011) 544–549, https://doi.org/10.1016/J.BBRC.2011.05.041.

[44] M. Bai, Dimerization of G-protein-coupled receptors: roles in signal transduction, Cell. Signal. 16 (2004) 175–186, https://doi.org/10.1016/S0898-6568(03)00128-1.

[45] M. F, B. H, B. J, F. JP, M. G, B. MT, C.-M. X, G. L, Bradykinin receptors: Agonists, antagonists, expression, signaling, and adaptation to sustained stimulation, Int. Immunopharmacol. 82 (2020), https://doi.org/10.1016/J.INTIMP.2020.106305.

[46] G.W. Zamponi, K.P.M. Currie, Regulation of CaV2 calcium channels by G protein coupled receptors, Biochim. Biophys. Acta 1828 (2013) 1629, https://doi.org/10.1016/J.BBAMEM.2012.10.004.

[47] C. WA, F. AP, Calcium channel regulation and presynaptic plasticity, Neuron. 59 (2008) 882–901, https://doi.org/10.1016/J.NEURON.2008.09.005.

[48] K. AE, Z. GW, Presynaptic calcium channels: structure, regulators, and blockers, Handb. Exp. Pharmacol. 184 (2008) 45–75, https://doi.org/10.1007/978-3-540-74805-2_3.

[49] Y. E, E. T, S. T, Angiotensin II-induced inhibition of calcium currents via G(q/11)-protein involving protein kinase C in hamster submandibular ganglion neurons, Neurosci. Res. 43 (2002) 179–189, https://doi.org/10.1016/S0168-0102(02)00039-1.

[50] E. H, L. SG, M. M, S. T, B. S, Presynaptic inhibition of transmitter release from rat sympathetic neurons by bradykinin, J. Neurochem. 93 (2005) 1110–1121, https://doi.org/10.1111/J.1471-4159.2005.03084.X.

[51] M.D. V, R. SS, R. J, Growth hormone secretagogue receptor constitutive activity impairs voltage-gated calcium channel-dependent inhibitory neurotransmission in hippocampal neurons, J. Physiol. 596 (2018) 5415–5428, https://doi.org/10.1113/JP276256.

[52] L.S. EJ, A. F, C. A, M. ER, D. VM, G. MA, R. S, C. D, F. R, P. M, R. J, Constitutive and ghrelin-dependent GHSR1a activation impairs CaV2.1 and CaV2.2 currents in hypothalamic neurons, J. Gen. Physiol. 146 (2015) 205–219, https://doi.org/10.1085/JGP.201511383.

[53] E.R. Mustafá, E.J.L. Soto, V.M. Damonte, S.S. Rodríguez, D. Lipscombe, J. Raingo, Constitutive activity of the Ghrelin receptor reduces surface expression of voltage-gated Ca2+ channels in a CaVβ-dependent manner, J. Cell Sci. 130 (2017) 3907–3917, https://doi.org/10.1242/jcs.207886.

[54] A. Fas, L.S. Easj, C. Aas, C. Das, S. Hasb, P. Mas, R. Jas, Melanocortin 4 receptor activation inhibits presynaptic N-type calcium channels in amygdaloid complex neurons, Eur. J. Neurosci. 40 (2014) 2755–2765, https://doi.org/10.1111/EJN.12650.

[55] M. CI, C.-F. C, R. SS, Y. A, D. C, R. J, Constitutive activity of dopamine receptor type 1 (D1R) increases CaV2.2 currents in PFC neurons, J. Gen. Physiol. 152 (2020), https://doi.org/10.1085/JGP.201912492.

[56] R.M. Evans, H. You, S. Hameed, C. Altier, A. Mezghrani, E. Bourinet, G. W. Zamponi, Heterodimerization of ORL1 and opioid receptors and its consequences for N-type calcium channel regulation *, J. Biol. Chem. 285 (2010) 1032–1040, https://doi.org/10.1074/JBC.M109.040634.

[57] C.G. S, M. ER, R. SS, P. M, R. J, Dopamine receptor type 2 and ghrelin receptor coexpression alters Ca V 2.2 modulation by G protein signaling cascades, ACS Chem. Neurosci. 11 (2020) 3–13, https://doi.org/10.1021/ACSCHEMNEURO.9B00426.

[58] M. ER, C.G. S, D. M, C. S, D. S, W. R, S. HB, F. JA, B. JL, P. M, R. J, LEAP2 impairs the capability of the growth hormone secretagogue receptor to regulate the dopamine 2 receptor signaling, Front. Pharmacol. 12 (2021), https://doi.org/10.3389/FPHAR.2021.712437.

[59] T. Takezako, H. Unal, S.S. Karnik, K. Node, The non-biphenyl-tetrazole angiotensin AT 1 receptor antagonist eprosartan is a unique and robust inverse agonist of the active state of the AT 1 receptor, Br. J. Pharmacol. 175 (2018) 2454–2469, https://doi.org/10.1111/bph.14213.

[60] J. Bian, J. Lei, X. Yin, P. Wang, Y. Wu, X. Yang, L. Wang, S. Zhang, H. Liu, M.L. X. Fu, Limited AT1 receptor internalization is a novel mechanism underlying sustained vasoconstriction induced by AT1 receptor autoantibody from preeclampsia, J. Am. Heart Assoc. 8 (2019), https://doi.org/10.1161/JAHA.118.011179.

[61] S. AbdAlla, H. Lother, U. Quitterer, AT 1-receptor heterodimers show enhanced G-protein activation and altered receptor sequestration, Nat. (2000) 4076800, 407 (2000) 94–98, https://doi.org/10.1038/35024095.

[62] U. Quitterer, X. Fu, A. Pohl, K.M. Bayoumy, A. Langer, S. AbdAlla, Beta-arrestin1 prevents preeclampsia by downregulation of mechanosensitive AT1-B2 receptor heteromers, Cell 176 (2019) 318–333, e19, https://doi.org/10.1016/J.CELL.2018.10.050.

[63] W. Li, J. Sui, I.C. Huang, J.H. Kuhn, S.R. Radoshitzky, W.A. Marasco, H. Choe, M. Farzan, The S proteins of human coronavirus NL63 and severe acute respiratory syndrome coronavirus bind overlapping regions of ACE2, Virology. 367 (2007) 367–374, https://doi.org/10.1016/J.VIROL.2007.04.035.

[64] P. S, G. T, W. A, P. K, van der H. L, B. B, H. H, Interaction between the spike protein of human coronavirus NL63 and its cellular receptor ACE2, Adv. Exp. Med. Biol. 581 (2006) 281–284, https://doi.org/10.1007/978-0-387-33012-9_47.

[65] S. Wang, F. Guo, K. Liu, H. Wang, S. Rao, P. Yang, C. Jiang, Endocytosis of the receptor-binding domain of SARS-CoV spike protein together with virus receptor ACE2, Virus Res. 136 (2008) 8–15, https://doi.org/10.1016/j.virusres.2008.03.004.

[66] H. Wang, P. Yang, K. Liu, F. Guo, Y. Zhang, G. Zhang, C. Jiang, SARS coronavirus entry into host cells through a novel clathrin- and caveolae-independent endocytic pathway, Cell Res. 18 (2008) 290–301, https://doi.org/10.1038/cr.2008.15.

[67] T.T. Cao, R.W. Mays, M. von Zastrow, Regulated endocytosis of G-protein-coupled receptors by a biochemically and functionally distinct subpopulation of clathrin-coated pits *, J. Biol. Chem. 273 (1998) 24592–24602, https://doi.org/10.1074/JBC.273.38.24592.

[68] S.-L. K, L. MD, E. HH, C. BR, Engineered G protein coupled receptors reveal independent regulation of internalization, desensitization and acute signaling, BMC Biol. 3 (2005), https://doi.org/10.1186/1741-7007-3-3.

[69] B.D. Cerrato, O.A. Carretero, B. Janic, H.E. Grecco, M.M. Gironacci, Heteromerization between the bradykinin B2 receptor and the angiotensin-(1–7) Mas receptor, Hypertension. 68 (2016) 1039–1048, https://doi.org/10.1161/HYPERTENSIONAHA.116.07874.

[70] J. Enquist, C. Sandén, C. Skröder, S.A. Mathis, L.M.F. Leeb-Lundberg, Kinin-dtimulated B1 receptor signaling depends on receptor endocytosis whereas B2 receptor signaling does not, Neurochem. Res. 396 (2013), https://doi.org/10.1007/S11064-013-1126-9, 39 (2013) 1037–1047.

[71] A. AU, T. MI, A. SD, A. M, Z. Z, H. H, S. A, A. G, Coronavirus disease 2019 (COVID-19): an overview of the immunopathology, serological diagnosis and management, Scand. J. Immunol. 93 (2021), https://doi.org/10.1111/SJI.12998.

[72] M. Duarte, F. Pelorosso, L.N. Nicolosi, M. Victoria Salgado, H. Vetulli, A. Aquieri, F. Azzato, M. Castro, J. Coyle, I. Davolos, I.F. Criado, R. Gregori, P. Mastrodonato, M.C. Rubio, S. Sarquis, F. Wahlmann, R.P. Rothlin, Telmisartan for treatment of Covid-19 patients: an open multicenter randomized clinical trial, EClinicalMedicine. 37 (2021) 100962, https://doi.org/10.1016/j.eclinm.2021.100962.

[73] A. Kamyshnyi, I. Krynytska, V. Matskevych, M. Marushchak, O. Lushchak, Arterial hypertension as a risk comorbidity associated with covid-19 pathology, Int. J. Hypertens. 2020 (2020), https://doi.org/10.1155/2020/8019360.

[74] L. Ren, S. Yu, W. Xu, J.L. Overton, N. Chiamvimonvat, P.N. Thai, Lack of association of antihypertensive drugs with the risk and severity of COVID-19: a meta-analysis, J. Cardiol. 77 (2021) 482–491, https://doi.org/10.1016/J.JJCC.2020.10.015/ATTACHMENT/B79E0804-23AC-47E4-8505-012C1FAC0FD4/MMC1.PDF.

[75] C. Gao, Y. Cai, K. Zhang, L. Zhou, Y. Zhang, X. Zhang, X. Zhang, Q. Li, W. Li, S. Yang, X. Zhao, Y. Zhao, H. Wang, Y. Liu, Z. Yin, R. Zhang, R. Wang, M. Yang, C. Hui, W. Wijns, J.W. Mcevoy, O. Soliman, Y. Onuma, P.W. Serruys, L. Tao, F. Li, Association of hypertension and antihypertensive treatment with COVID-19 mortality: a retrospective observational study, Eur. Heart J. 41 (2020) 2058–2066, https://doi.org/10.1093/EURHEARTJ/EHAA433.

[76] F. Yan, F. Huang, J. Xu, P. Yang, Y. Qin, J. Lv, S. Zhang, L. Ye, M. Gong, Z. Liu, J. Wei, T. Xie, K.F. Xu, G.F. Gao, F.S. Wang, L. Cai, C. Jiang, Antihypertensive drugs are associated with reduced fatal outcomes and improved clinical characteristics in elderly COVID-19 patients, Cell Discov. 61 (2020) 1–10, https://doi.org/10.1038/s41421-020-00221-6, 6 (2020).

[77] D.S. Ojeda, M.M.G. Lopez Ledesma, H.M. Pallarés, G.S. Costa Navarro, L. Sanchez, B. Perazzi, S.M. Villordo, D.E. Alvarez, M. Echavarria, K.Y. Oguntuyo, C.S. Stevens, B. Lee, J. Carradori, J.J. Caramelo, M.J. Yanovsky, A.V. Gamarnik, Y. Long-Ueira, M.L. Polo, M. Salvatori, S. Azzolina, Y. Ghiglione, H. Salomon, M.F. Quiroga, G. Turk, N. Laufer, Emergency response for evaluating SARS-CoV-2 immune status, seroprevalence and convalescent plasma in Argentina, PLoS Pathog. 17 (2021), https://doi.org/10.1371/journal.ppat.1009161.

[78] J. Schindelin, I. Arganda-Carreras, E. Frise, V. Kaynig, M. Longair, T. Pietzsch, S. Preibisch, C. Rueden, S. Saalfeld, B. Schmid, J.-Y. Tinevez, D.J. White, V. Hartenstein, K. Eliceiri, P. Tomancak, A. Cardona, Fiji: an open-source platform for biological-image analysis, Nat. Methods 97 (2012) 676–682, https://doi.org/10.1038/nmeth.2019, 9 (2012).

[79] T.M. Beasley, R.E. Schumacher, Multiple regression approach to analyzing contingency tables: post hoc and planned comparison procedures, J. Exp. Educ. 64 (1995) 79–93, https://doi.org/10.1080/00220973.1995.9943797.

[80] M.A. García-Pérez, V.V. Núñez-Antón, Cellwise residual analysis in two-way contingency tables, Educ. Psychol. Meas. 63 (2003) 825–839, https://doi.org/10.1177/0013164403251280.